NANO LETTERS

2007
Vol. 7, No. 6
1827−1831

Fluorescent Ion-Selective Nanosensors for Intracellular Analysis with Improved Lifetime and Size

J. Matthew Dubach, Daniel I. Harjes, and Heather A. Clark*

Bioengineering Group, The Charles Stark Draper Laboratory, 555 Technology Square, Cambridge, Massachusetts 02139

Received April 3, 2007; Revised Manuscript Received April 30, 2007

ABSTRACT

We describe the synthesis and characterization of sodium-selective polymeric nanosensors that improves upon the lifetime and size of previous fiberless nanosensors. Sonication is used to form the polymer nanospheres that contain all the components needed for ion sensing. Even though the size is small (approximately 120 nm), the lifetime of these sensors in solution is on the order of a week. The surface coating has also been optimized for stability, biocompatibility, and ease of chemical modification.

Much of our knowledge of intracellular ion signaling has focused predominantly on calcium, indisputably important in many of the fundamental processes of life.[1] The advent of molecular probes for imaging calcium in single cells provided information on spatial dynamics that would not otherwise have been attained with other ion measurement techniques such as whole cell patch-clamp.[2,3] In addition, high-throughput analysis, essential for drug screening, has also been made possible through the use of these probes.[4,5] Since indicators available for other physiological ions, such as sodium and potassium, have not found the same utility, the question remains as to the importance of these ions in signaling. We know that sodium and potassium are essential in the beat of the heart and the firing of a synapse, but little is known about their spatial dynamics, with only a few instances of hot spots or channel clustering being reported.[6,7]

Fluorescent nanosensors, or PEBBLEs, were first created to extend the range of fluorescent indicators that could be used for intracellular measurements by creating a biocompatible shell around the dyes.[8,9] The real power of particle-based nanosensors was realized when PEBBLEs based on ion-selective optodes were first introduced by the Kopelman group.[10−12] These elegant sensors combined the versatility of ion-selective optical sensors with the size and biocompatibility requirements of intracellular ion measurements. The benefits of the decyl methacrylate-based nanosensors were numerous; they were submicron, spherical, fluorescent, and exquisitely selective for the ion of interest. In addition, the range of measurement was tunable to maximize sensitivity at physiological ranges. The only drawbacks were that these early sensors were time-consuming to make, suffered from short lifetimes in solution, and were slightly large for intracellular work, ranging from a reported 500 nm to 1 μm in diameter.[10]

In this study, we describe the synthesis and characterization of ion-selective polymeric nanosensors that improve upon the lifetime and size of previous[10−12] liquid polymer nanosensors. Our goal was to make the system easier to produce in the laboratory, lengthen the lifetime of the sensors in solution, and make the whole sensor smaller. We use three basic components in our system; molecular indicators that make the ion-extraction principle work, a plasticized polymer matrix, and a biocompatible coating.

The core of the sensor is composed of a standard optode matrix, which contains plasticized poly(vinyl chloride), chromoionopore, ionophore, and a negative lipophilic additive. The nanosensor was made more biocompatible and stable in aqueous solution by including a surface modifier that coats the nanosensor. The modifier is an amphiphilic molecule that readily inserts into the hydrophobic sensor, leaving the hydrophilic, biocompatible component on the outside of the sensor exposed to the aqueous environment. The sensors are formed by addition of the optode in a 50:50 solution of tetrahydrofuran and dichloromethane to an aqueous solution under intense sonication. The surface modifier is dissolved in the aqueous solution and inserts into the nanosensor during formation. Figure 1a shows an idealized image of the nanosensor coated with the surface modifier. The surface modifier used in Figure 1 is a PEG-lipid, however, others were explored as well. The ability of the lipid tail to insert into the nanosensor and remain stable demonstrates the possibility of surface modification for future experiments. Theoretically, any chemistry linked to a lipid tail could be attached to the surface of the nanosensor.

* Corresponding author. E-mail: hclark@draper.com.

10.1021/nl0707860 CCC: $37.00
Published on Web 05/11/2007

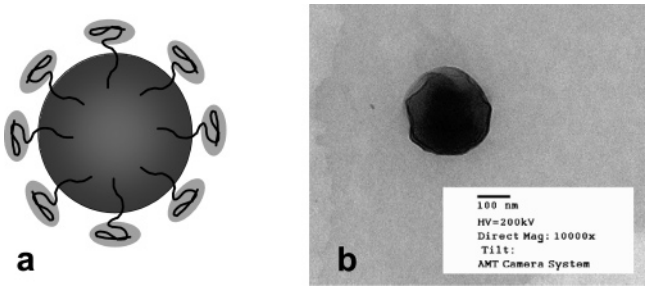

Figure 1. Poly(ethylene glycol) coating of the nanosensor. (a) A cartoon depiction of a nanosensor coated by PEG-lipid molecules. The lipid tail of the molecule inserts into the nanosensor leaving the PEG group to stabilize the sensor in an aqueous solution. (b) A TEM image of a PEG-lipid coated nanosensor. The nanosensor is ~180 nm, which is approximately one standard deviation of the average nanosensor size.

Dynamic light scattering was performed to analyze the size and distribution of the nanosensors. The average size using 200 μg of PEG-lipid as the surface modifier was 123 $\pm$ 44 nm, as measured with a particle sizer. The technique was consistent, with an RSD of 2.4%. All sensors were smaller than 220 nm, after filtration through a standard filter to remove larger particles. TEM images were obtained in order to confirm the size, and an example of a 180 nm particle is shown in Figure 1b. Currently, we have no size tunability, although conceivably changes in the solvent ratio used could give us some small degree of control. Other experiments, shown below, confirmed that the nanosensors are stable in an aqueous solution and do not aggregate.

The amount of surface modifier necessary to achieve stability in solution was analyzed. PEG-lipid was added during the formulation of the nanosensors at different concentrations, and the diameter and zeta potential were determined, Figure 2a. Both the size, reported in diameter, and the zeta potential increased as more PEG-lipid was added. The zeta potential, a measure of surface charge, became more negative, and therefore the nanosensors became more stable in the aqueous solution. The increase in size was not drastic, but was expected as a greater amount of PEG-lipid coated more surface area of the nanosphere. It was observed that nanosensors with no coating aggregated due to hydrophobicity of the polymer so a zero PEG-lipid concentration was not included in these studies. Both size and zeta potential show an exponential decay response to increasing amounts of PEG-lipid. The size of the nanosensors remained constant past 200 μg, while the zeta potential became constant just beyond that concentration. At 200 μg of PEG-lipid, the nanosensors were optimally coated and remained separated in an aqueous suspension. Stability of the nanosensors in solution, the critical determinant when considering coatings, was analyzed by measuring the size of the sensors 2 days after formation, Figure 2b. At this time, size of the nanosensors significantly increased at the lower concentrations of PEG-lipid. However, at 200 μg, the size remained fairly constant. The slight increase may be due to further incorporation of PEG-lipid into the nanosensor, but the sensors showed no signs of aggregation. We found no further size changes in the stable suspensions after 2 days. On the basis of these results, 200 μg of PEG-lipid was used as the surface modifier throughout the rest of the experiments unless it is otherwise noted.

The relative amounts of the individual components necessary for the optode to function were altered until an ideal response curve was generated. The component concentrations were derived from previous publications using similar components and theoretical values found from established equations defining optode function.[13−15] The ratios of the components control the concentration range of the nanosensors as well as the resolution within this range. In this case, the nanosensors were designed to monitor sodium at physiologically relevant levels. The intracellular sodium concentration is roughly 10 mM for most cells. Therefore, a sensor with a half-maximal response centered on this value will have a higher resolution at physiologically relevant concentrations. The composition used for these sensors produced a concentration range with a half-maximal response of ~20 mM, determined by fitting a sigmoidal curve to the data plotted

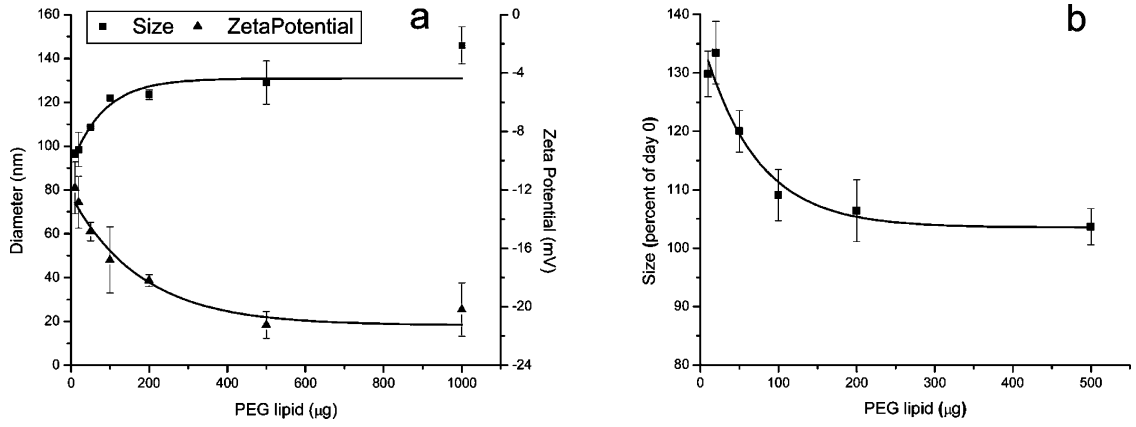

Figure 2. The size and zeta potential of the nanosensors were determined with varying concentrations of PEG-lipid. (a) The size (squares) is reported as the diameter of the nanosensor and the zeta potential (triangles) is reported in millivolts. Both represent an average and standard deviation of three separate batches. (b) The change in size of the nanosensors 2 days after formation. The data represent an average plus standard deviation of three measurements from one batch of nanosensors at each PEG-lipid concentration. Data are shown as percent change of the diameter of the nanosensor from day 0 to day 2.

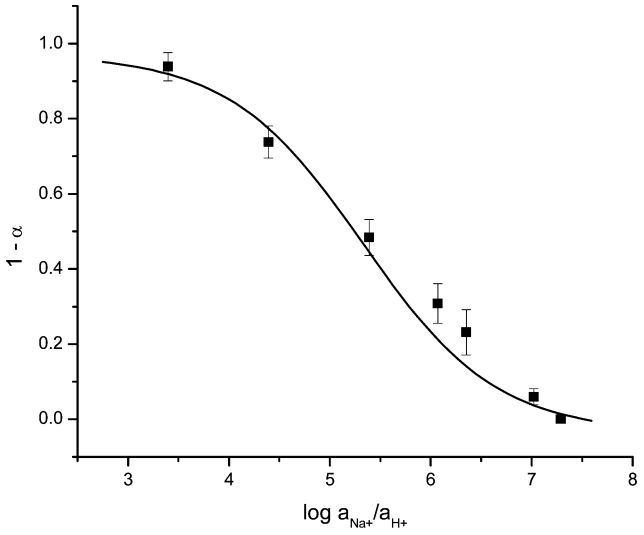

Figure 3. The response of the nanosensors to sodium. The nanosensors were diluted in a buffered solution and subsequent additions of sodium were made to obtain the calibration curve. The data are represented as $1 - \alpha$, where $\alpha = (I_{max} - I_{[Na+]})/(I_{max} - I_{min})$, $I_{[Na+]}$ is the intensity (excite 570, emit 680) at the concentration of sodium being measured and I_{min} and I_{max} are the intensities at zero sodium and 1 M sodium, respectively. A theoretical response curve is also shown (solid black line). The data shown were obtained from the nanosensors during 8 days after formation and represent the average and standard deviation of five separate calibrations.

in Figure 3 (fit curve not shown). The data are represented as $1 - \alpha$, as previously defined by:[15]

$$\alpha = (I_{max} - I_{[Na+]})/(I_{max} - I_{min}) \quad (1)$$

where $I_{[Na+]}$ is the intensity at the concentration of sodium being measured and I_{min} and I_{max} are the intensities at zero sodium and 1 M sodium, respectively. The theoretical response curve for the nanosensors is also plotted in Figure 3; this is based on an equation described previously by Tsagkatakis et al.[15] The data were generated by taking the average and standard deviation of five calibrations over the course of 8 days from one batch of nanosensors and were repeatable through multiple batches.

Here we define the resolution of the nanosensors to be the change in sodium concentration from the intracellular concentration capable of producing a 1% change in fluorescent signal on the instrument with which the sensors were calibrated. This value correlates to the steepness of a linear fit of the calibration curve at 10 mM sodium and is a good indication of the ability of the nanosensors to detect relevant concentration changes resulting from sodium signaling. The resolution of the sensor in this range, based on a sigmoidal curve fit to the data, is 370 μM. As a physiological point of reference, astrocytes have been reported to produce changes of 20−30 mM in sodium concentration.[16] Other cells do not produce such drastic concentration changes; however, the sensors are capable of providing spatial resolution when used with microscopy, allowing localized sodium responses that are higher than total cell sodium concentrations for excitable cells.

The dynamics of sodium signaling of cells are quite fast—sodium channels open for mere milliseconds. Thus, to follow a channel opening in real-time, both the sensor response time and the instrument acquisition time must be kept small. Because of the small size of the sensors (~120 nm diameter), the response time to sodium is estimated to be on the order of microseconds.[10,17] To obtain fast acquisition times, it is not realistic for the instrument, such as a confocal microscope, to make a ratiometric measurement because the time it takes to switch between two wavelengths can be cumbersome and dividing the emission onto multiple detectors reduces the signal-to-noise, a critical parameter when acquiring rapidly. Thus, while a ratiometric calibration gives comparable calibrations and is superior for a quantitative measurement, for our purposes, we chose to calibrate using a single wavelength.

The nanosensors were also tested in parallel for selectivity over potassium. Potassium is much more prevalent inside

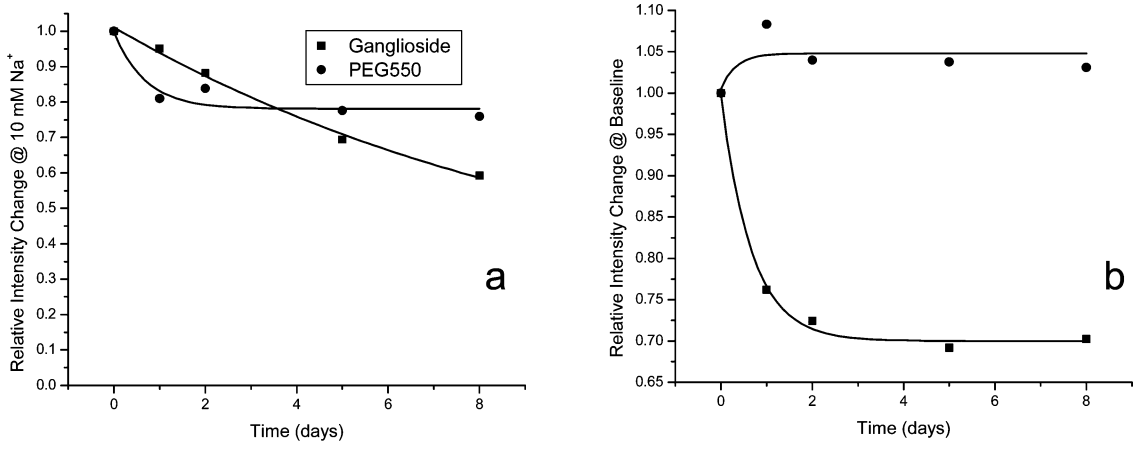

Figure 4. Lifetime of the nanosensors and the effects of component leaching. The lifetime was determined by running calibrations on the nanosensors over the course of 8 days. Two surface modifiers were used; total brain ganglioside (squares) and PEG 550 lipid (circles). (a) The intensity values (excite 570, emit 680) obtained at a sodium concentration of 10 mM were compared to the original intensity of the nanosphere at day 0 and plotted. The values were extracted from the calibration curve generated for each experiment. (b) The intensity of the sensors at baseline, or zero sodium. The degree of chromoionophore leaching was determined from this plot.

the cell (~140 mM) than sodium. However, addition of potassium showed no measurable response up to 1 M. In other words, the nanosensors are completely selective for sodium over potassium for intracellular concentrations. A similar result was previously shown in a study using the same sodium ionophore in plasticized PVC.[15] The selectivity for sodium over potassium in that case was 2.5 orders of magnitude. This would be just barely detectable in the concentrations that were explored and confirms the selectivity determined here.

One of the major improvements of the sensors demonstrated in this study is the lifetime in solution. Optodes are prone to component leaching, which limits the ability to respond accurately and repetitively.[18] As the size of the optode becomes smaller, the surface area to volume ratio increases and the amount of component leaching also increases. The additive is the component that most readily leaches due to its lower lipophilicity. Other additives were explored but were unable to produce better results. Figure 4a shows the ability of the nanosensors to produce repeatable responses to sodium concentration over the course of 8 days in solution. Initially, there was a slight decrease in the response at 10 mM, but for the PEG-lipid coated nanosensors, the decrease leveled off and the sensors produced the same response. Interestingly, coating the sensors with a different surface modifier, total ganglioside extract, did not prevent leaching, perhaps indicating that the synthesized PEG-lipid provides a barrier that allows the sensors to retain the components after the slight initial loss.

The original intensity of the sensors does not change over time for the PEG-lipid coated nanosensors, Figure 4b. This implies that the chromoionophore itself is not leaching out of the sensor. However, the sodium concentration required to achieve half-maximal response slightly decreases over the time period, shown in Figure 4a. This is reflected by the standard deviation seen in Figure 3 as well. Therefore, one of the components is slightly leaching, and the change in the response over time indicates that it is indeed the additive. The slight degree of additive leaching that is seen, however, is not as destructive as it might be imagined. In most cellular ion measurement experiments, a calibration is performed at the end to allow the conversion of fluorescent signal to ion concentration. This procedure would eliminate the effects of the minor leaching that occurs when the sensors are used over extended periods of time.

The nanosensors in this study also showed ideal biocompatibility. The cytotoxicity was determined by incubating the nanosensors overnight with HEK 293 cells and measuring the degree of cellular injury with an MTT assay. These results were compared to other nanoparticles and are shown in Figure 5. The sodium nanosensors show no cellular toxicity compared to controls over the course of 72 h after incubation. This result is also seen for 100 nm diameter gold nanoparticles, which were used as a positive control due to their generally accepted biocompatibility. Twenty nm latex spheres were used as a negative control for the assay. The 100 nm spheres of the same variety and surface chemistry showed no negative effects and thus were not shown. This size effect

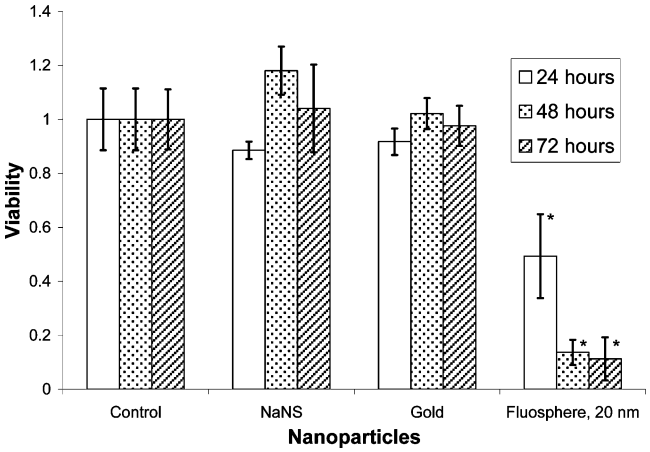

Figure 5. Biocompatibility of the nanosensors. The nanosensors were incubated with HEK 293 cells in culture and an MTT assay was performed 24, 48, and 72 h postincubation. The experiments were carried out in groups of 8 for control, nanosensors, gold nanoparticles, and fluospheres. The data were compared to the control for each time series and the average and standard deviation were plotted. $p < 0.01$ compared to control denoted by $*$.

served well as a negative control for the assay, giving an indication of assay robustness.

In summary, we present here an improved model for an intracellular sodium nanosensor based on optode technology. The sensors were tuned to achieve an ideal response to intracellular sodium concentrations. They have a lifetime in solution of over a week and were shown to be biocompatible. Future work will explore the uses of these sensors in measuring sodium response in cells. These new sensors will allow intracellular sodium measurements similar to those of calcium, thus advancing the field of sodium signaling and detection.

Acknowledgment. This work made use of the MRSEC Shared Experimental Facilities at MIT, supported by the National Science Foundation under award number DMR-02-13282.

Supporting Information Available: Materials and methods. This material is available free of charge via the Internet at http://pubs.acs.org.

References

(1) Rudolf, R.; Mongillo, M.; Rizzuto, R.; Pozzan, T. *Nat. Rev. Mol. Cell. Biol.* **2003**, *4*, 579−586.
(2) Williams, D. A.; Fogarty, K. E.; Tsien, R. Y.; Fay, F. S. *Nature* **1985**, *318*, 558−561.
(3) Wier, W. G.; Cannell, M. B.; Berlin, J. R.; Marban, E.; Lederer, W. J. *Science* **1987**, *235*, 325−328.
(4) DeBernardi, M. A.; Brooker, G. *Methods Enzymol*. **2006**, *414*, 317−35.
(5) Gribbon, P.; Chambers, C.; Palo, K.; Kupper, J.; Mueller, J.; Sewing, A. *J. Biomol. Screen* **2006**, *11*, 511−518.
(6) Massensini, A. R.; Suckling, J.; Brammer, M. J.; Moraes-Santos, T.; Gomez, M. V.; Romano-Silva, M. A. *J. Neurosci. Methods* **2002**, *116*, 189−196.
(7) Koh, D. S.; Jonas, P.; Vogel, W. *J. Physiol.* **1994**, *479*, 183−197.
(8) Clark, H. A.; Hoyer, M.; Philbert, M. A.; Kopelman, R. *Anal. Chem.* **1999**, *71*, 4831−4836.
(9) Clark, H. A.; Tjalkens, R.; Philbert, M. A.; Kopelman, R. *Anal. Chem.* **1999**, *71*, 4837−4843.

(10) Brasuel, M.; Kopelman, R.; Miller, T. J.; Tjalkens, R.; Philbert, M. A. *Anal. Chem.* **2001**, *73*, 2221−2228.
(11) Brasuel, M. G.; Miller, T. J.; Kopelman, R.; Philbert, M. A. *Analyst* **2003**, *128*, 1262−1267.
(12) Brasuel, M.; Kopelman, R.; Kasman, I.; Miller, T. J.; Philbert, M. A. *Proc. IEEE* **2002**, *1*, 288−292.
(13) Johnson, R. D.; Bachas, L. G. *Anal. Bioanal. Chem.* **2003**, *376*, 328−41.
(14) Buhlmann, P.; Pretsch, E.; Bakker, E. *Chem. Rev.* **1998**, *98*, 1593−1688.
(15) Tsagkatakis, L.; Peper, S.; Retter, R.; Bell, M.; Bakker, E. *Anal. Chem.* **2001**, *73*, 6083−6087.
(16) Bernardinelli, Y.; Magistretti, P. J.; Chatton, J. Y. *Proc. Natl. Acad. Sci. U.S.A.* **2004**, *101*, 14937−14942.
(17) Bakker, E.; Buhlmann, P.; Pretsch, E. *Chem. Rev.* **1997**, *97*, 3083−3132.
(18) Qin, Y.; Bakker, E. *Anal. Chem.* **2003**, *75*, 6002−6010.

NL0707860